RING PATTERNS AND THEIR BIFURCATIONS IN A NONLOCAL MODEL OF BIOLOGICAL SWARMS

Andrea L. Bertozzi, James von Brecht and Hui Sun

Department of Mathematics, University of California
Los Angeles, CA, 90095-1555, USA

Theodore Kolokolnikov

Department of Mathematics and Statistics, Dalhousie University
Halifax, Nova Scotia, B3H3J5, Canada

David Uminsky

Department of Mathematics, University of San Francisco
San Francisco, CA, 94117-1080, USA

Abstract. In this paper we study the pattern formation of a kinematic aggregation model for biological swarming in two dimensions. The swarm is represented by particles and the dynamics are driven by a gradient flow of a non-local interaction potential which has a local repulsion long range attraction structure. We leverage a co-dimension one formulation of the continuum gradient flow to characterize the stability of ring solutions for general interaction kernels. In the regime of long-wave instability we show that the resulting ground state is as a low mode bifurcation away from the ring and use weakly nonlinear analysis to provide conditions for when this bifurcation is a pitchfork. In the regime of short-wave instabilities we show that the rings break up into fully 2D ground states in the large particle limit. We analyze the dependence on the stability of a ring on the number of particles and provide examples of complex multi-ring bifurcation behavior as the number of particles increases. We are also able to provide a solution for the "designer potential" problem in 2D. Finally, we characterize the stability of the rotating rings in the second order kinetic swarming model.

1. **Introduction.** Mathematical models for swarming, schooling, and other aggregative behavior in biology have given us many tools to understand the fundamental behavior of collective motion and pattern formation that occurs in nature [10, 6, 2, 26, 25, 14, 7, 13, 27, 19, 33, 32, 23, 11, 17, 37, 38, 34, 36, 9, 15, 29, 21, 20, 24, 8]. One of the key features of many of these models is that the social communication between individuals (sound, chemical detection, sight, etc...) is performed over different scales and are inherently nonlocal [11, 22, 2]. In the case of swarming, these nonlocal interactions between indviduals usually consist of a shorter range repulsion to avoid collisions and medium to long range attraction to keep the swarm
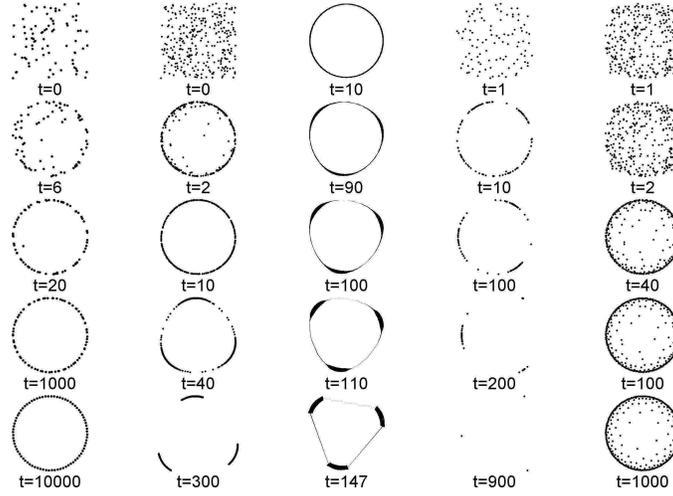
FIGURE 1. Dynamics of (2). First column: $f(r) = 1 - r$, $N = 80$. The equilibrium solution is a stable ring. Second column: $f(r) = r^{-0.5} - r^5$, $N = 300$. Third column: Simulation of the continuum limit (4) with F as in the second column. Fourth column: $f(r) = 1 - r^{2.2}$, $N = 100$. Fifth column: $f(r) = r^{-0.5} - r^{0.5}$, $N = 300$.

cohesive. While some models include anisotropy in this communication (e.g. an organism's eyes may have a limited field of vision) simplified isotropic interactions have been shown to capture many important swarming behaviors including milling [20, 10]. More recently it has been shown [17, 38, 37] that the competition between the desire to avoid collisions and the desire to remain in a cohesive swarm can sometimes result in simple radially symmetric patterns such as rings, annuli and uniform circular patches and other times result in exceedingly complex patterns. Moreover how modelers select the strength and form of the repulsion near the origin has a direct effect on the co-dimension of the swarm [1]. In particular, the possible co-dimensionality of the ground state is directly related to the singularity of the interaction kernel at the origin.

The focus of this paper is to develop an understanding of which patterns will form (in 2D) in a given swarm as a function of the nonlocal social interaction. The goal is to develop tools that can help us predict when a swarm will aggregate into a ring or an annulus or some other complex ground state from a given model for there social interactions. The classical approach to understanding pattern formation (say in PDEs), first suggested in Turing [35], is to perform a careful stability analysis around a homogeneous state and to determine the unstable modes. In the case of classic Turing instabilities driven by diffusion the resulting unstable Fourier modes sometimes characterize the final ground state pattern (e.g. stripes and spots) in the solution. To understand patterns driven, not by diffusion, but nonlocal repulsion-attraction interactions such as the ones found in Figure 1, we take a similar approach.

To develop a theory for predicting the final ground state formation of a swarm, we formulate our pattern as extrema of the N-particle pairwise, interaction energy

$$E(\mathbf{x}_1, \ldots, \mathbf{x}_N) = \sum_{i, j \neq i} P(|\mathbf{x}_i - \mathbf{x}_j|) \tag{1}$$

where P denotes the isotropic pairwise interaction potential. We consider the associated gradient flow to the interaction energy (1) which takes the form

$$\frac{\mathrm{d}\mathbf{x}_i}{\mathrm{d}t} = -\nabla_{\mathbf{x}_i} E = \frac{1}{N} \sum_{\substack{j=1 \ldots N \\ j \neq i}} f\left(|\mathbf{x}_i - \mathbf{x}_j|\right) (\mathbf{x}_i - \mathbf{x}_j), \quad i = 1 \ldots N, \tag{2}$$

where $f(r) = F(r)/r$ and $F(r) = -P'(r)$ is the force associated to our potential P.

We will be able to characterize the patterns seen in Figure 1 by employing a stability analysis of equation (1) but unlike classical Turing patterns, we will linearize around uniform ring solutions. The instabilities of these co-dimension one, radially symmetric solutions nicely characterize the resulting ground state even when we the resulting pattern is not co-dimension one.

We will make use of the underlying continuum formulation of (2) known as the aggregation equation [17, 18, 3, 4] which takes the form

$$\rho_t(\mathbf{x}, t) + \nabla \cdot (\rho(\mathbf{x}, t)\mathbf{u}(\mathbf{x}, t)) = 0, \quad \mathbf{x} \in \mathbb{R}^3, \ t \geq 0$$

$$\mathbf{u}(\mathbf{x}, t) = \int_{\mathbb{R}^3} f\left(|\mathbf{x} - \mathbf{y}|\right) (\mathbf{x} - \mathbf{y}) \rho(\mathbf{y}, t) \, \mathrm{d}\mathbf{y}. \tag{3}$$

Here, ρ describes the density of particles and $\mathbf{u}$ is the velocity field. By then considering a weak formulation of (3) where the density aggregates on a co-dimension one curve one can derive, see [30, 17, 38] the evolution equation for the material point of the curve, $\mathbf{Y}(\boldsymbol{\xi})$, to be

$$\mathbf{y}_t = \mathbf{u} = \int_D f(|\mathbf{y} - \mathbf{y}'|)(\mathbf{y} - \mathbf{y}')\rho_0(\boldsymbol{\xi}')\mathrm{d}\mathcal{S}_{\boldsymbol{\xi}'}, \tag{4}$$

where we parameterize the curve with Lagrangian parameter $\boldsymbol{\xi} \in D \subset \mathbb{R}^1$.

We now summarize the results in this paper. In section 2 we derive the characterization of the stability of the ring solution. In section 3 we use asymptotic techniques to give a characterization of stability with respect to high-order modes. When the high modes are unstable, the ring breaks up completely; the resulting steady state may be an annulus or more complex two-dimensional shapes such as shown in the last column of Figure 1. In section 4 we analyze a family of power law interaction kernels using the stability theory and provide bifurcation diagrams. In section 5 we analyze the deformation of a ring due to low mode instability near the bifurcation point using weakly nonlinear analysis. At the level of the particle system, the transition from a ring to an annulus is described in detail in section 6. For a specific class of kernels, we identify a critical number N_c, which we compute asymptotically, such that the ring is stable when $N < N_c$ and is unstable otherwise. In contrast to high mode-instabilities, the low-mode instabilities can deform the ring while preserving the curve-type structure. In section 7 we solve a restricted inverse problem: given an instability of a certain mode, design the kernel f which leads to such an instability in the ground state. Finally in section 8 we extend our analysis to second order models of self-propelled particles considered in [20, 10] to characterize the stability of a rotating ring.

Some of the results in this paper already appeared elsewhere. The statements of results of sections 2, 4, 5 appeared previously in a shorter form in [17] but without proofs. Here, we provide the detailed derivations of these calculations. The three and higher-dimensional analogue of a ring and its stability was also solved in [38] using a different technique that relies on spherical harmonics. The results on custom kernels in section 7 are based on ideas first presented in [37], where the same problem was solved in three dimensions. We include the two-dimensional case here for completeness. Results in Section 6 and 8 have not appeared elsewhere and are new to this paper.

2. **Stability of ring solutions.** We begin by considering the ring steady state for the equations (2) consisting of N particles equally spaced particles located on a ring of radius R,

$$x_j = R\exp\left(2\pi ij/N\right), \quad j = 1\ldots N.$$

The equilibrium value for R then satisfies

$$0 = \sum_{j=1}^{N-1} f(2R\sin(\pi j/N))(1 - e^{i2\pi j/N}); \tag{5}$$

in the continuum limit $N \to \infty$, this becomes

$$\int_0^{\frac{\pi}{2}} f(2R\sin\theta)\sin^2\theta d\theta = 0. \tag{6}$$

We can now analyze the stability of the ring equilibrium of radius R given from (6). Our first result is the following characterization of local stability.

Theorem 2.1. *In the continuum limit $N \to \infty$, consider the ring equilibrium of radius R given by (6) for the flow (4). Define*

$$I_1(m) := \frac{4}{\pi}\int_0^{\pi/2} \left(Rf'\left(2R\sin\theta\right)\sin\theta + f\left(2R\sin\theta\right)\right)\sin^2((m+1)\theta)d\theta; \tag{7}$$

$$I_2(m) := \frac{4}{\pi}\int_0^{\pi/2} \left(Rf'\left(2R\sin\theta\right)\sin\theta\right)\left[\sin^2(\theta) - \sin^2(m\theta)\right] d\theta; \tag{8}$$

$$M(m) := \begin{pmatrix} I_1(m) & I_2(m) \\ I_2(m) & I_1(-m) \end{pmatrix}. \tag{9}$$

Suppose that $\lambda \leq 0$ for all eigenvalues λ of $M(m)$ for all $m \in \mathbb{N}$. Then the ring equilibrium is locally stable. It is unstable otherwise.

For finite N, the ring is stable if $\lambda \leq 0$ for all eigenvalues λ of $M(m)$ for all $m = 1, 2, \ldots N$, but with I_1, I_2 as given by (17, 18) below.

An example of a stable ring is provided by interaction kernel $f(r) = 1 - r$. In this case a straightforward computation yields

$$R = \frac{3\pi}{16};$$

$$I_1(m) = -\frac{m^2 + 2m + 3}{(1 + 2m)(3 + 2m)}; \quad I_1(-m) = \begin{cases} -\dfrac{m^2 - 2m + 3}{(1 - 2m)(3 - 2m)}, & m \neq 1 \\ 0, & m = 1 \end{cases}$$

$$I_2(m) = -\frac{m^2 - 1}{4m^2 - 1},$$

so that, for $m > 1$, we have

$$\det M(m) = \frac{12m^2(2m^2 - 1)}{(1 - 4m^2)^2 (4m^2 - 9)} > 0, \quad \operatorname{trace} M(m) = \frac{9 + 4m^2 - m^2}{(1 - 4m^2)(4m^2 - 9)} < 0.$$

This shows that the eigenvalues corresponding to $m > 1$ are all negative. Similarly, the eigenvalues corresponding to mode $m = 0, 1$ are also stable. Moreover, for large m, the two eigenvalues are $\lambda \sim -\frac{1}{4}$ and $\lambda \sim -\frac{3}{8m^2} \to 0$ as $m \to \infty$. The presence of small eigenvalues implies the existence of slow dynamics near the ring equilibrium. Further analysis shows that the eigenvector corresponding to the small eigenvalue and large m is nearly tangential to the circle; the other eigenvector is nearly perpendicular. The corresponding two-time dynamics are also clearly visible in simulations (Figure 1, column 1).

Proof of Theorem 2.1. Consider the perturbations of the ring of N particles of the form

$$x_j = R \exp(2\pi i j/N)(1 + h_j) \quad \text{with} \quad h_j \ll 1. \tag{10}$$

We compute

$$x_j - x_k = R \exp(2\pi i k/N) \left(1 - e^{i\phi} + h_j - e^{i\phi}h_k\right) \quad \text{where} \quad \phi = \frac{2\pi(k - j)}{N}.$$

$$|x_k - x_j| \sim 2R \left|\sin\frac{\phi}{2}\right| + \frac{R}{4\left|\sin\frac{\phi}{2}\right|}\left[(1 - e^{i\phi})\left(h_k + \overline{h_j}\right) + (1 - e^{-i\phi})\left(\overline{h_k} + h_j\right)\right].$$

Substituting (10) into (2) leads to the following linearized system,

$$\frac{dh_j}{dt} = \sum_k f'\left(2R\left|\sin\frac{\phi}{2}\right|\right) \frac{R}{4\left|\sin\frac{\phi}{2}\right|}[(1 - e^{i\phi})\left(h_k + \overline{h_j}\right)$$

$$+ (1 - e^{-i\phi})\left(\overline{h_k} + h_j\right)]\left(1 - e^{i\phi}\right)$$

$$+ \sum_k f\left(2R\left|\sin\frac{\phi}{2}\right|\right)\left(h_j - e^{i\phi}h_k\right), \quad \text{where } \phi = \frac{2\pi(k - j)}{N}.$$

Next we use the identities

$$(1 - e^{i\phi})^2 = -4\sin^2\left(\frac{\phi}{2}\right)e^{i\phi}; \quad (1 - e^{i\phi})(1 - e^{-i\phi}) = 4\sin^2\left(\frac{\phi}{2}\right)$$

to obtain

$$\frac{dh_j}{dt} = \sum_{k, k \neq j} G_1(\phi/2)\left(h_j - e^{i\phi}h_k\right) + G_2(\phi/2)\left(\overline{h_k} - e^{i\phi}\overline{h_j}\right),$$
$$\text{where } \phi = \frac{2\pi(k - j)}{N}, \tag{11}$$

with

$$G_1(\phi) = \frac{1}{N}Rf'\left(2R\left|\sin\phi\right|\right)\left|\sin\phi\right| + \frac{1}{N}f\left(2R\left|\sin\phi\right|\right);$$
$$G_2(\phi) = \frac{1}{N}Rf'\left(2R\left|\sin\phi\right|\right)\left|\sin\phi\right|. \tag{12}$$

Using the ansatz

$$h_j = \xi_+(t)e^{im\theta} + \xi_-(t)e^{-im\theta}, \quad \theta = 2\pi j/N, \quad m \in \mathbb{N}. \tag{13}$$

We can write

$$h_k = \xi_+ e^{im\theta}e^{im\phi} + \xi_- e^{-im\theta}e^{-im\phi}, \tag{14}$$

and substituting (13), (14) into (11) and collecting like terms in $e^{im\phi}, e^{-im\phi}$ leads to the system

$$\xi'_+ = \xi_+ \sum_{k,k\neq j} G_1(\phi/2) \left(1 - e^{i(m+1)\phi}\right) + \bar{\xi}_- \sum_{k,k\neq j} G_2(\phi/2) \left(e^{im\phi} - e^{i\phi}\right) \qquad (15)$$

$$\xi'_- = \xi_- \sum_{k,k\neq j} G_1(\phi/2) \left(1 - e^{i(-m+1)\phi}\right) + \bar{\xi}_+ \sum_{k,k\neq j} G_2(\phi/2) \left(e^{-im\phi} - e^{i\phi}\right). \qquad (16)$$

It is easy to check that the sums in (15, 16) are all real so that the system becomes

$$\xi'_+ = \xi_+ I_1(m) + \bar{\xi}_- I_2(m), \quad \bar{\xi}'_- = \bar{\xi}_- I_1(-m) + \xi_+ I_2(-m)$$

where

$$I_1(m) = \sum_{k,k\neq j} G_1(\phi/2) \left(1 - e^{i(m+1)\phi}\right) = 4 \sum_{k=1}^{N/2} G_1(\frac{\pi k}{N}) \sin^2 \left(\frac{(m+1)\pi k}{N}\right), \qquad (17)$$

$$I_2(m) = \sum_{k,k\neq j} G_2(\phi/2) \left(e^{im\phi} - e^{i\phi}\right)$$

$$= 4 \sum_{k=1}^{N/2} G_2(\frac{\pi k}{N}) \left[\sin^2 \left(\frac{\pi k}{N}\right) - \sin^2 \left(\frac{m\pi k}{N}\right)\right]. \qquad (18)$$

We thus obtain

$$\begin{pmatrix} \xi'_+ \\ \bar{\xi}'_- \end{pmatrix} = M \begin{pmatrix} \xi_+ \\ \bar{\xi}_- \end{pmatrix}$$

where M is given by (9). Finally, I_1 and I_2 are just the Riemann sums so that in the continuum limit $N \to \infty$, these sums are given by (7, 8). Substituting $\xi_\pm = b_\pm \exp(\lambda t)$ we find that λ is the eigenvalue of the matrix M. $\blacksquare$

3. **High wave-number stability.** We next examine the behaviour of the eigenvalues as $m \to \infty$, i.e. the high frequency wave limit. We shall call a ring *short-wave stable* if the eigenvalues corresponding to all sufficiently large modes m have negative real part; otherwise we call the ring *short-wave unstable*. Kernels that are short-wave unstable generally result in ground state patterns which are no longer co-dimension one as we will see in section 6. In contrast, short-wave stable kernels often contain low mode symmetries bifurcating away from the ring but otherwise remain a co-dimension one curve. For simplicity, we restrict ourselves to the case where $f(s)$ may be written as a generalized power series, although a similar result can be derived for a more general case where f is sufficiently smooth. Our main result is the following.

Theorem 3.1. *(Necessary and sufficient conditions for short-wave (in)stability) Suppose that $f(r)$ admits a generalized power series expansion in the form*

$$f(s) = a_0 s^{p_0} + a_1 s^{p_1} + \ldots, \qquad p_0 < p_1 < \ldots. \qquad (19)$$

Moreover, suppose that $p_0 > -3$ and $a_0 > 0$. Let p_l be the smallest power which is not even. Then following conditions are sufficient for the ring to be short-wave

stable:

$$p_0 > -1; \tag{20}$$

$$\int_0^{\pi/2} \left(Rf'\left(2R\sin\theta\right)\sin\theta + f\left(2R\sin\theta\right) \right) d\theta < 0; \tag{21}$$

either $a_l > 0$ *and* $p_l \in (-1, 0) \cup (1, 2) \cup (4, 6) \dots$
or $a_l < 0$ *and* $p_l \in (0, 1) \cup (2, 4) \cup (6, 8) \dots$ \hfill (22)

The ring is short-wave unstable if either $p_0 \leq -1$ *or the inequality in either (21) or (22) is reversed.*

Remark. We note that the condition $p_0 > -3$ is needed in order for the ring to exist; otherwise, the integral in (6) is undefined.

Proof. First, suppose that $-3 < p_0 \leq -1$. Then by Lemma A.1, we have that

$$I_1(m) \sim I_1(-m) \sim \begin{cases} Cm^{-p_0-1}, & p_0 \in (-3, -1) \\ C\ln m, & p_0 = -1 \end{cases} \quad \text{as } m \to \infty$$

where $C > 0$. In this case $\text{trace}(M(m)) \to +\infty$ as $m \to \infty$ so that $\lambda > 0$ for all m sufficiently large. Therefore we obtain (20) as the necessary condition for eventual stability of a ring. When (20) holds, we may estimate

$$I_1(m) \sim I_1(-m) \sim \frac{2}{\pi} \int_0^{\pi/2} \left(Rf'\left(2R\sin\theta\right)\sin\theta + f\left(2R\sin\theta\right) \right) d\theta$$

The necessary condition for stability is that $\text{trace}(M(m)) < 0$ as $m \to \infty$ or

$$\int_0^{\pi/2} \left(Rf'\left(2R\sin\theta\right)\sin\theta + f\left(2R\sin\theta\right) \right) d\theta < 0. \tag{23}$$

To establish sufficient conditions for eventual stability, we also require that $\det M > 0$ as $m \to \infty$. To simplify the computations we may assume, by rescaling the space, that $R = 1/2$ and write

$$I_1(\pm m) \sim I_{10} + I_{11}; \qquad I_2(\pm m) \sim I_{20} + I_{21}$$

with

$$I_{10} = \frac{2}{\pi} \int_0^{\pi/2} \left(\frac{1}{2} f'\left(\sin\theta\right)\sin\theta + f\left(\sin\theta\right) \right) d\theta;$$

$$I_{20} = \frac{2}{\pi} \int_0^{\pi/2} f'\left(\sin\theta\right)\left(\sin^3\theta - \frac{1}{2}\sin\theta \right) d\theta;$$

$$I_{11} = -\frac{2}{\pi} \int_0^{\pi/2} \left(\frac{1}{2} f'\left(\sin\theta\right)\sin\theta + f\left(\sin\theta\right) \right) \cos(2m\theta) d\theta;$$

$$I_{21} = \frac{2}{\pi} \int_0^{\pi/2} \frac{1}{2} f'\left(\sin\theta\right)\sin\theta \cos(2m\theta) d\theta;$$

Next, using (6) and integration by parts, we note the following identity:

$$\int_0^{\pi/2} f(\sin\theta)d\theta = \int_0^{\pi/2} f(\sin\theta)\left(1 - \sin^2\theta\right)d\theta$$

$$= \int_0^{\pi/2} f(\sin\theta)\cos\theta\frac{d}{d\theta}\sin\theta d\theta$$

$$= \int_0^{\pi/2} f'(\sin\theta)\left(\sin^3\theta - \sin\theta\right)d\theta.$$

It follows that $I_{10} = I_{20}$. Therefore we obtain

$$\det M \sim 2I_{10}\left(I_{11} - I_{21}\right)$$

Now from Lemma A.1 we have the following identity:

$$\int_0^{\pi/2} \sin^p(x)\sin(2mx)dx \sim -\sin\left(\frac{\pi p}{2}\right)c(p)m^{-p-1} \quad \text{as} \quad m \to \infty; \quad p > -1$$

$$\text{where} \quad c(p) = \frac{1}{2\sqrt{\pi}}\Gamma\left(\frac{p}{2} + \frac{1}{2}\right)\Gamma(\frac{p}{2} + 1)$$

Using the series expansion (19), we then obtain

$$I_{11} - I_{21} \sim -a_l\left(1 - p_l\right)c(p_l)\sin\left(\pi\frac{p_l}{2}\right)m^{-p_l-1}$$

where l is such that p_l is the smallest non-even power in the generalized power series expansion (19). Now by assumption (20), we have $p_l > -1$ and also note that

$$\left(1 - p_l\right)c(p_l)\sin\left(\pi\frac{p_l}{2}\right) < 0, \quad \text{if} \quad p_l \in (-1,0) \cup (1,2) \cup (4,6)\ldots$$

$$> 0, \quad \text{if} \quad p_l \in (0,1) \cup (2,4) \cup (6,8)\ldots$$

Assuming $I_{10} < 0$, we have $\det M > 0$ provided that (22) holds.

4. **Power force law.** In this section, we present more explicit results for the force where the attraction and repulsion are given by power laws. That is, we consider the interaction force $F(r) = r^p - ar^q$, corresponding to

$$f(r) = r^{p-1} - ar^{q-1} \quad \text{with} \quad p < q, \quad a > 0. \tag{24}$$

The constant a can be scaled out, and so it does not affect stability. For convenience, we will choose a such that the ring radius is precisely $R = \frac{1}{2}$. From (6) we then obtain:

$$a = \frac{\int_0^{\pi/2} \sin^{p+1}\theta d\theta}{\int_0^{\pi/2} \sin^{q+1}\theta d\theta} = \frac{\Gamma\left(1 + p/2\right)\Gamma(3/2 + q/2)}{\Gamma(3/2 + p/2)\Gamma\left(1 + q/2\right)}.$$

We also evaluate

$$\int_0^{\pi/2} \left(Rf'\left(2R\sin\theta\right)\sin\theta + f\left(2R\sin\theta\right)\right)d\theta$$

$$= \frac{p+1}{2}\int_0^{\pi/2} \sin^{p-1}\theta d\theta - a\frac{q+1}{2}\int_0^{\pi/2} \sin^{q-1}\theta d\theta$$

$$= (p-q)(pq-1)\frac{\sqrt{\pi}\Gamma(p/2)}{8\Gamma(3/2 + p/2)}.$$

From Theorem 3.1, it follows that the ring is short-wave stable provided that that $pq > 1$ and $p > 0$.
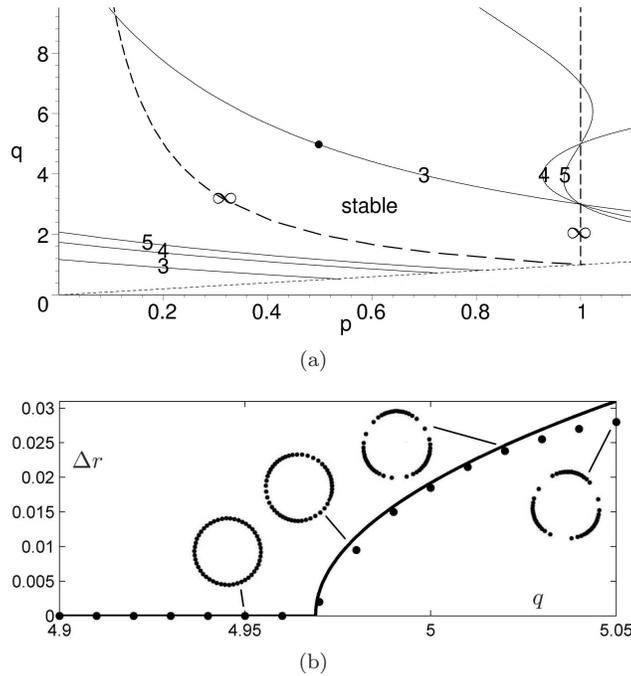
(a)

(b)

FIGURE 2. (a) Stability region of a ring solution for the force law
(24). Instability boundaries corresponding to $m = 3, 4, 5$ and $m =
\infty$ are indicated. Crossing any of these boundaries triggers the
corresponding instability. The stable region is bounded by the
instability of mode 3 from above the curve $pq = 1$ (corresponding
to instabilities of modes $m \rightarrow \infty$) from below. (b) Bifurcation
diagram for interaction force (24) near the dot shown in (a), with
$p = 0.5$, and as q is varied. The solid curve is derived from weakly
nonlinear analysis while the dots are simulations of (2).

Next, we compute $\det(M(m))$, using the key integral (A.1) derived in the Appendix. Omitting the details, we obtain the following polynomial expressions for when $\det(M(m)) = 0$, for the low modes $m = 2, 3, \ldots$:

$$m = 2 : 7 + 38(p + q) + 12pq + 3(p^2 + q^2) + 2\left(pq^2 + p^2q\right) - p^2q^2 = 0$$

$$\begin{aligned} m = 3 : &\ 723 - 594(p + q) - 27(p^2 + q^2) - 431pq + 106\left(pq^2 + p^2q\right) \\ &+ 19\left(p^3q + pq^3\right) + 10\left(p^3q^2 + p^2q^3\right) + 6\left(p^3 + q^3\right) + p^3q^3 = 0. \end{aligned}$$

The instability thresholds for modes $m \geq 4$ can be analogously computed, each resulting in a symmetric polynomial in p, q of degree $2m$. Each of these polynomials corresponds to the stability boundary of mode m. Using Maple, we have plotted each of these boundaries for $m = 2, 3, 4, 5$, as well as the stability boundary $pq = 1$ for large modes m. These are shown in Figure 2(a).

5. **Weakly nonlinear Analysis: Low mode bifurcations.** Theorem 2.1 characterizes the conditions for a ring solution to be stable in the limit $N \rightarrow \infty$. That is, the eigenvalues of the matrix $M(m)$ defined in (9) must be both non-positive. For a

given mode m, when one of the eigenvalues becomes zero, the stability changes. In this section, we study the general bifurcation dynamics near a ring solution using weakly nonlinear analysis. As such, we take the continuum limit of (2) as described in [30]:

$$x'(\theta, t) = \frac{1}{2\pi} \int_0^{2\pi} f(\nu, |x(\theta, t) - x(\underset{\sim}{\theta}, t)|)(x(\theta, t) - x(\underset{\sim}{\theta}, t))\mathrm{d}\underset{\sim}{\theta}, \qquad (25)$$

where ν is considered to be the bifurcation parameter and $x'(\theta, t)$ denotes $\partial x(\theta, t)/\partial t$. We are particularly interested in the critical value of ν, i.e. $\nu = \nu_0$, which yields a zero determinant of $M(m)$, with the corresponding ring steady state solution

$$x(\theta, t) = u_0(\theta, t) = Re^{i\theta}. \qquad (26)$$

For the sake of brevity, in the rest of this section we use the notation x for $x(\theta, t)$, $\underset{\sim}{x}$ for $x(\underset{\sim}{\theta}, t)$, f for $f(\nu_0, |x(\theta, t) - x(\underset{\sim}{\theta}, t)|)$, $\partial_\nu f$ for $\partial f/\partial\nu$ evaluated at $(\nu_0, |x(\theta, t) - x(\underset{\sim}{\theta}, t)|)$, and f', f'', etc. for the corresponding derivatives of f with respect to the second argument evaluated at $(\nu_0, |x(\theta, t) - x(\underset{\sim}{\theta}, t)|)$.

Let $0 \le \epsilon \ll 1$ be an expansion parameter near a bifurcation point u_0,

$$x(\theta, t) = u_0(\theta, t) + \epsilon u_1(\theta, t) + \epsilon^2 u_2(\theta, t) + \epsilon^3 u_3(\theta, t) + \cdots, \qquad (27)$$

$$\nu = \nu_0 + \epsilon\nu_1 + \epsilon^2\nu_2 + \cdots. \qquad (28)$$

At order $O(\epsilon)$, we obtain the linear equation

$$\begin{aligned} \mathcal{L}(u_1, \bar{u}_1) =& \frac{1}{\pi} \int_0^\pi (f'R\sin\Delta\theta + f)(u_1 - \underset{\sim}{u_1})\mathrm{d}\Delta\theta \\ &- \frac{e^{2i\theta}}{\pi} \int_0^\pi f'R\sin\Delta\theta e^{2i\Delta\theta}(\bar{u}_1 - \underset{\sim}{\bar{u}_1})\mathrm{d}\Delta\theta \\ =& -\nu_1 I_0 e^{i\theta}, \text{ with } I_0 = \frac{4}{\pi} \int_0^{\pi/2} R\partial_\nu f \sin^2\Delta\theta\mathrm{d}\Delta\theta \end{aligned} \qquad (29)$$

and $\Delta\theta = (\underset{\sim}{\theta} - \theta)/2$. The solution to (29) is $u_1 = b_1 e^{i(m+1)\theta} + b_2 e^{-i(m-1)\theta} + b_0 e^{i\theta}$, where $[b_1, b_2]^t \in \mathcal{N}(M(m))$ and $b_0 = \nu_1 c_1$, with $c_1 = -I_0/(I_1(0) + I_2(0))$. This is the eigenvalue problem for the linear stability of the ring solution. Typically one measures the amplitude that the solution deviates either radially as $|b_2 + b_1|$ or tangentially as $|b_2 - b_1|$.

At order $O(\epsilon^2)$, we obtain

$$\begin{aligned} \mathcal{L}(u_2, \bar{u}_2) =& \\ &- \nu_1 (b_1, b_2) \cdot \begin{pmatrix} 2c_1 I_3(m) + \partial_\nu I_1(m) & -2c_1 I_4(m) + \partial_\nu I_2(m) \\ -2c_1 I_4(m) + \partial_\nu I_2(m) & 2c_1 I_3(-m) + \partial_\nu I_1(-m) \end{pmatrix} \cdot \begin{pmatrix} e^{i(m+1)\theta} \\ e^{-i(m-1)\theta} \end{pmatrix} \\ &- \begin{pmatrix} b_1^2 I_5(m) + b_2^2 I_6(m) - b_1 b_2 I_7(m) \\ b_1^2 I_5(-m) + b_2^2 I_6(-m) - b_1 b_2 I_7(-m) \end{pmatrix}^t \cdot \begin{pmatrix} e^{i(2m+1)\theta} \\ e^{-i(2m-1)\theta} \end{pmatrix} \\ &- \left(\nu_2 I_0 + \frac{\nu_1^2}{2}\partial_\nu I_0 + \left(b_1 b_2 I_4(m) + b_1^2 I_3(m) + b_2^2 I_3(-m)\right)\right) e^{i\theta}, \end{aligned}$$

$$(30)$$

where

$$I_3(m) = \frac{4}{\pi} \int_0^{\pi/2} (2Rf'' \sin \Delta\theta + 3f'^2(m+1)\Delta\theta \sin \Delta\theta \mathrm{d}\Delta\theta,$$

$$I_4(m) = \frac{4}{\pi} \int_0^{\pi/2} (2Rf'' \sin \Delta\theta + f') \sin (m-1)\Delta\theta \sin (m+1)\Delta\theta \sin \Delta\theta \mathrm{d}\Delta\theta,$$

$$I_5(m) = \frac{2}{\pi} \int_0^{\pi/2} (\frac{3}{2}f' + Rf'' \sin \Delta\theta) \sin^2 (m+1)\Delta\theta \sin (2m+1)\Delta\theta \mathrm{d}\Delta\theta,$$

$$I_6(m) = \frac{2}{\pi} \int_0^{\pi/2} (-\frac{1}{2}f' + Rf'' \sin \Delta\theta) \sin^2 (m-1)\Delta\theta \sin (2m+1)\Delta\theta \mathrm{d}\Delta\theta,$$

$$I_7(m) = \frac{2}{\pi} \int_0^{\pi/2} (3f' + 2Rf'' \sin \Delta\theta) \sin (m-1)\Delta\theta \sin (m+1)\Delta\theta \sin (2m+1)\Delta\theta \mathrm{d}\Delta\theta.$$

Applying the Fredholm alternative to ensure that the right hand side of (30) is in the range space of the linear operator $\mathcal{L}$ determines a unique solution $u_2 = b_1^2 c_3 e^{i(2m+1)\theta} + b_1^2 c_4 e^{-i(2m-1)\theta} + (\nu_2 c_1 + b_1^2 c_2)e^{i\theta}$, subject to the condition that $\nu_1 = 0$, where

$$c_2 = -\frac{-I_1(m)I_4(m)/I_2(m) + I_3(m) + I_1(m)^2 I_3(-m)/I_2(m)^2}{I_1(0) + I_2(0)},$$

$$\begin{bmatrix} c_3 \\ c_4 \end{bmatrix} = -M(2m)^{-1} \cdot \begin{bmatrix} I_5(m) + I_1(m)^2 I_6(m)/I_2(m)^2 + I_1(m)I_7(m)/I_2(m) \\ I_5(-m) + I_1(m)^2 I_6(-m)/I_2(m)^2 + I_1(m)I_7(-m)/I_2(m) \end{bmatrix} \tag{31}$$

Finally, at $O(\epsilon^3)$, we use the equation $\mathcal{L}(u_3, \bar{u}_3) = \mathcal{R}_3(u0, u1, u2, \nu2)$, to determine the relation between ν_2 and b_1, b_2. Applying the Fredholm alternative to this equation,

$$\mathrm{Im}\left(\mathcal{R}_3(u0, u1, u2, \nu2)(I_1(m)e^{-i(m+1)\theta} + I_2(m)e^{i(m-1)\theta})\right) = 0, \tag{32}$$

which yields

$$\nu_2 = \kappa b_1^2$$

$$\kappa = \frac{\tau_4 I_1(m)I_2(m) - \tau_3 I_2(m)^2}{\tau_1 I_2(m) - \tau_2 I_1(m) + I_2(m)^2 \partial_\nu I_1(m) - 2I_1(m)I_2(m)\partial_\nu + I_1(m)^2 \partial_\nu I_1(-m)}, \tag{33}$$

where

$$\tau_1 = 2c_1 I_2(m)I_8(m) + 2c_1 I_1(m)I_9(m)$$

$$\tau_2 = -2c_1 I_1(m)I_8(-m) - 2c_1 I_2(m)I_9(m)$$

$$\tau_3 = 2c_2 I_8(m) + 2c_2 I_1(m)I_9(m)/I_2(m)$$
$$\quad + c_3 I_1(m)I_{11}(m)/I_2(m) + c_3 I_{10}(m) + c_4 I_1(m)I_{11}(-m)/I_2(m) + c_4 I_{12}(-m)$$
$$\quad + I_{14}(m) + I_1(m)I_{15}(m)/I_2(m) + I_1(m)^2 I_{16}(m)/I_2(m)^2 + I_1(m)^3 I_{13}(-m)/I_2(m)^3$$

$$\tau_4 = -2c_2 I_1(m)I_8(-m)/I_2(m) - 2c_2 I_9(m)$$
$$\quad - c_4 I_{11}(-m) - c_4 I_1(m)I_{10}(-m)/I_2(m) + c_3 I_1(m)I_{11}(m)/I_2(m) + c_3 I_{12}(m)$$
$$\quad - I_1(m)^3 I_{14}(-m)/I_2(m)^3 - I_1(m)^2 I_{15}(-m)/I_2(m)^2 - I_1(m)I_{16}(-m)/I_2(m) - I_{13}(m)$$
$$\tag{34}$$

and

$$I_8(m) = \frac{2}{\pi} \int_0^{\pi/2} (2Rf'' \sin \Delta\theta + 3f') \sin^2 (m+1)\Delta\theta \sin \Delta\theta \mathrm{d}\Delta\theta,$$

$$I_9(m) = \frac{2}{\pi} \int_0^{\pi/2} (2Rf'' \sin \Delta\theta + f') \sin (m-1)\Delta\theta \sin (m+1)\Delta\theta \sin \Delta\theta \mathrm{d}\Delta\theta,$$

$$I_{10}(m) = \frac{2}{\pi} \int_0^{\pi/2} (2Rf'' \sin \Delta\theta + 3f') \sin^2 (m+1)\Delta\theta \sin (2m+1)\Delta\theta \mathrm{d}\Delta\theta,$$

$$I_{11}(m) = \frac{2}{\pi} \int_0^{\pi/2} (2Rf'' \sin \Delta\theta + 3f') \sin (m-1)\Delta\theta \sin (m+1)\Delta\theta \sin (2m+1)\Delta\theta \mathrm{d}\Delta\theta,$$

$$I_{12}(m) = \frac{2}{\pi} \int_0^{\pi/2} (2Rf'' \sin \Delta\theta + f') \sin^2 (m-1)\Delta\theta \sin (2m+1)\Delta\theta \mathrm{d}\Delta\theta,$$

$$I_{13}(m) = \frac{2}{\pi} \int_0^{\pi/2} (2Rf''' \sin \Delta\theta + 3f'' - \frac{3f'}{2R\sin\Delta\theta}) \sin (m-1)\Delta\theta \sin^3 (m+1)\Delta\theta \mathrm{d}\Delta\theta,$$

$$I_{14}(m) = \frac{2}{\pi} \int_0^{\pi/2} (2Rf''' \sin \Delta\theta + 5f'' + \frac{3f'}{2R\sin\Delta\theta}) \sin^4 (m+1)\Delta\theta \mathrm{d}\Delta\theta,$$

$$I_{15}(m) = \frac{2}{\pi} \int_0^{\pi/2} (\frac{5}{3}Rf''' \sin \Delta\theta + 2f'' - \frac{f'}{R\sin\Delta\theta}) \sin^3 (m+1)\Delta\theta \sin (m-1)\Delta\theta \mathrm{d}\Delta\theta,$$

$$I_{16}(m) = \frac{2}{\pi} \int_0^{\pi/2} (\frac{5}{3}Rf''' \sin \Delta\theta + 2f'' + \frac{f'}{R\sin\Delta\theta}) \sin^2 (m-1)\Delta\theta \sin^2 (m+1)\Delta\theta \mathrm{d}\Delta\theta.$$

$$(35)$$

These calculations allow us to summarize this section with the following theorem:

Theorem 5.1. *Let $f(\nu, r)$ be an attractive-repulsive kernel, with a parameter ν, where mode m perturbation is stable for $\nu < \nu_0$, unstable for $\nu > \nu_0$ and $f(\nu_0, r)$ gives the instability threshold $\det(M(m)) = 0$. Given the following conditions:*

1. $I_0 \neq 0$
2. $I_1(0) + I_2(0) \neq 0$
3. *The matrix* $N(m) = \begin{pmatrix} 2c_1 I_3(m) + \partial_\nu I_1(m) & -2c_1 I_4(m) + \partial_\nu I_2(m) \\ -2c_1 I_4(m) + \partial_\nu I_2(m) & 2c_1 I_3(-m) + \partial_\nu I_1(-m) \end{pmatrix}$ *has nonzero determinant.*
4. *The matrix $M(2m)$ has nonzero determinant.*
5. *The denominator of κ in (33) is nonzero.*

Then we have a pitchfork bifurcation for solutions of (25) at $\nu = \nu_0$, with bifurcation coefficient defined as either

$$\nu_2/|b_1 + b_2|^2 = \kappa I_2(m)^2/(I_1(m) - I_2(m))^2 \quad \text{(radially),} \quad \text{or}$$

$$\nu_2/|b_1 - b_2|^2 = \kappa I_2(m)^2/(I_1(m) + I_2(m))^2 \quad \text{(tangentially),}$$

where ν_2 and κ are defined in (33).

With this theorem, we are able to say that the bifurcation type for the kernel $f(\nu, r) = r^{-0.5} - \nu r^{\nu-1}$ at $\nu_0 \approx 4.9696$ is pitchfork with bifurcation coefficient $\nu_2/|b_1 + b_2|^2 \approx 84.18$. We can see the details of the pitchfork bifurcation in Figure 2, also refer to [17]. In contrast, we can re-examine the stability of collapsing rings with power law $f(r) = r^{\nu-2}$, with $\nu > 2$, studied in [31]. We can conclude that this is not a pitchfork bifurcation and moreover it is condition (4) in theorem 5.1 that is
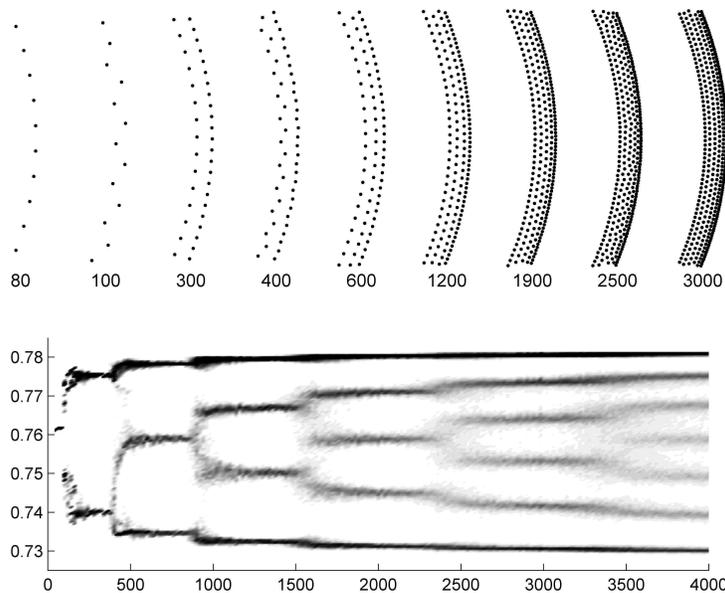
FIGURE 3. Bifurcations of a ring into multiple rings as a function of N, using $f(r) = 1 - r^2 + 0.35/r$. Top: steady states with N as indicated. These were computed by evolving (2) starting from random initial conditions. A part of the annulus-type solution is shown at $t = 25,000$. Bottom: The bifurcation diagram with N on the horizontal axis. The vertical axis shows the distribution of the radii of the particles obtained by computing a steady state up to $t = 5000$ using random initial conditions.

not satisfied. Whenever $M(m)$ has zero determinant, $M(2m)$ has zero determinant as well. In this situation, the stable scaled ring solution collapses sharply to clusters that form vertices of a regular simplex once the bifurcation parameter ν passes its critical value.

6. **High mode bifurcations: ring to annulus.** In Theorem 3.1 we characterized the stability of the ring with respect to high modes. In particular, we showed that if $f(r) = O(r^p)$ as $r \to 0$, then $p > -1$ is the first necessary condition. A natural question is what kind of bifurcation can occur when this condition fails. To answer this question, we concentrate on the following function $f(r)$:

$$f(r) = f_0(r) + \frac{1}{r}\delta \quad \text{with } \delta \ll 1, \tag{36}$$

where we assume that (36) with $\delta = 0$ admits a stable ring solution. In particular, we assume that $f_0(r)$ satisfies the conditions of Theorem 3.1 to guarantee short-wave stability of a ring when $\delta = 0$. To motivate the discussion, Figure 3 shows a numerical computation of the steady state for $f(r) = r - 1 + \frac{\delta}{r}$ for several values of N and with $\delta = 0.35$. Note that when $N = 80$, the steady state appears to converge to a simple ring solution, which on the surface appears to contradict the condition (20) of Theorem 3.1. This discrepancy is due to the finiteness of N. Indeed, when N is increased to 100, the steady state consisting of two rings begins to emerge. As

N is increased further, complex patterns emerge consisting of more and more rings. The bifurcation to $k-$ring pattern appears to take place when the mode $m = N/k$ first becomes unstable. We start by characterizing the first such transition, when the two-ring pattern first bifurcates from a single ring. We summarize the result as follows.

Proposition 1. *Suppose that $f(r)$ is given by (36). Let $N = N_c$ be given by*

$$N_c = \frac{\pi}{4} \exp\left(\frac{\alpha}{\delta} - \gamma - 1\right) \tag{37}$$

where

$$\alpha := -4R \int_0^{\pi/2} \left(Rf_0'(2R\sin\theta)\sin\theta + f_0(2R\sin\theta)\right)d\theta \tag{38}$$

and where R satisfies (6). Then the ring is stable for all $N < N_c$ and is unstable for $N > N_c$. More explicitly, we have

$$N_c \sim \frac{\pi}{4} \exp(\alpha_1 - \gamma - 1) \exp\left(\frac{\alpha_0}{\delta}\right) \tag{39}$$

where $\alpha = \alpha_0 + \delta\alpha_1 + O(\delta^2)$ with

$$\alpha_0 = -\int_0^{\pi/2} 4R_0^2 f_0'(2R_0\sin\theta)\sin\theta + 4R_0 f_0(2R_0\sin\theta)\,d\theta \tag{40}$$

$$\alpha_1 = -\int_0^{\pi/2} 16R_0R_1 f_0'(2R\sin\theta)\sin\theta + 8R_0^2 R_1 f_0''(2R_0\sin\theta)\sin^2\theta + 4R_1 f_0(2R\sin\theta)\,d\theta \tag{41}$$

and $R = R_0 + \delta R_1 + O(\delta^2)$ with

$$0 = \int_0^{\pi/2} f_0(2R_0\sin\theta)\sin^2(\theta); \tag{42}$$

$$0 = \frac{1}{2R_0} + 2R_1 \int_0^{\pi/2} f_0'(2R_0\sin\theta)\sin^3(\theta). \tag{43}$$

In the limit $N \to \infty$, the steady state consisting of a thin annulus eventually forms, as illustrated in Figure 3. These numerical simulations also suggest that the width of such an annulus appears to be well-approximated by the width of the double-ring solution that first arises when N crosses N_c. The distance between the two rings of such a solution can be asymptotically computed as follows.

Proposition 2. *Using the notation as in Proposition 1, suppose $\alpha > 0$. Then in the large N limit the particle system admits a double-ring steady state consisting of two rings of radii $R - \varepsilon$ and $R + \varepsilon$ with*

$$\varepsilon \sim 4eR \exp\left(-\alpha/\delta\right) \tag{44}$$

$$\sim 4eR_0 \exp\left(-\alpha_1\right) \exp\left(-\alpha_0/\delta\right). \tag{45}$$

Before proving Propositions 1 and 2, consider the following example:

$$f(r) = 1 - r + \delta/r.$$

Formulas (40) to (43) yield

$$R_0 = \frac{3\pi}{16}; \ R_1 = \frac{2}{\pi}; \ \alpha_0 = \frac{3\pi^2}{64}; \ \alpha_1 = 5$$

so that (39) and (45) then yields

$$N_c \sim \frac{\pi}{4} e^{4-\gamma} \exp\left(\frac{3\pi^2}{64\delta}\right); \quad \varepsilon \sim \frac{3\pi}{4} e^{-4} \exp\left(-\frac{3\pi^2}{64\delta}\right) \quad \text{as} \ \ \delta \to 0. \quad (46)$$

Taking $\delta = 0.35$, this yields $N_c \sim 90.29$ and $2\varepsilon \sim 0.01975$. A more accurate estimate, valid to all algebraic orders in δ, is given by (37, 44) and yields $N_c \sim 80.63$ and $2\varepsilon \sim 0.03331$. This agrees very well with full numerical simulation of the flow (2) as Figure 3 demonstrates: taking $N = 80$, random initial conditions were observed to converge to a ring solution; on the other hand, the double-ring structure is clearly visible when $N = 100$. Moreover, the distance between the inner and outer ring of the resulting annulus is about 0.03, in line with the theoretical prediction of $2\varepsilon \sim 0.033$.

Proof of Proposition 1. Using the notation of Theorem 2.1, we recall that

$$I_1(m-1) = 4 \sum_{k=1}^{N/2} G_1(\frac{\pi k}{N}) \sin^2\left(\frac{m\pi k}{N}\right), \quad (47)$$

$$I_2(m) = 4 \sum_{k=1}^{N/2} G_2(\frac{\pi k}{N}) \left[\sin^2\left(\frac{\pi k}{N}\right) - \sin^2\left(\frac{m\pi k}{N}\right)\right]. \quad (48)$$

We set $m = \frac{N}{2}$ in (47); then $\sin^2\left(\frac{m\pi k}{N}\right) = \sin^2\left(\frac{\pi k}{2}\right) = \begin{cases} 0, & k \ \text{even} \\ 1, & k \ \text{odd} \end{cases}$ so that (47) becomes

$$I_1(m-1) = 4 \sum_{\substack{k \ \text{odd}}}^{N/2} G_1(\frac{\pi k}{N}) = I_{10} + I_{11}$$

where we define

$$I_{10} = \frac{4}{N} \sum_{\substack{k \ \text{odd}}}^{N/2} Rf_0'\left(2R\left|\sin\frac{\pi k}{N}\right|\right) \left|\sin\frac{\pi k}{N}\right| + f_0\left(2R\left|\sin\frac{\pi k}{N}\right|\right); \quad I_{11} = \frac{\delta}{NR} \sum_{\substack{k \ \text{odd}}}^{N/2} \frac{1}{\sin\frac{\pi k}{N}}. \quad (49)$$

We estimate

$$I_{10} \sim \frac{2}{\pi} \int_0^{\pi/2} \left(Rf_0'\left(2R\sin\theta\right)\sin\theta + f_0\left(2R\sin\theta\right)\right) d\theta$$

and to isolate the singularity in I_{11} we write

$$I_{11} = \frac{\delta}{NR} \sum_{\substack{k \ \text{odd}}}^{N/2} \left(\frac{1}{\sin\frac{\pi k}{N}} - \frac{N}{\pi k}\right) + \frac{\delta}{\pi R} \sum_{\substack{k \ \text{odd}}}^{N/2} \frac{1}{k}.$$

Next, we use the identity

$$\sum_{k=0}^{M} \frac{1}{2k+1} = \frac{1}{2}\ln M + \frac{\gamma}{2} + \ln(2) + O(M^{-1})$$

and approximate

$$\frac{2}{N} \sum_{\substack{k \ \text{odd}}}^{N/2} \left(\frac{1}{\sin\frac{\pi k}{N}} - \frac{N}{\pi k}\right) \sim \frac{1}{\pi} \int_0^{\pi/2} \left(\frac{1}{\sin(\theta)} - \frac{1}{\theta}\right) d\theta = \frac{1}{\pi}\left(2\ln 2 - \ln\pi\right)$$

so that

$$I_{11} \sim \frac{\delta}{2\pi R} \left(\ln N + \ln(4/\pi) + \gamma \right).$$

Similarly, we find that

$$I_2 = 4 \sum_{k=1}^{N/2} G_2(\frac{\pi k}{N}) \sin^2 \left(\frac{\pi k}{N} \right) - 4 \sum_{k \text{ odd}}^{N/2} G_2(\frac{\pi k}{N}) = I_{20} + I_{21}$$

where

$$I_{20} \sim \frac{2}{\pi} \int_0^{\pi/2} Rf'(2R\sin\theta) 2\sin^3\theta - Rf_0'(2R\sin\theta)\sin\theta d\theta; \qquad (50)$$

$$I_{21} = I_{11}. \qquad (51)$$

Next we further simplify I_{20} as follows. From (6) we have

$$\int_0^{\pi/2} f_0(2R\sin\theta)\sin^2\theta d\theta = -\frac{\delta}{2R} \qquad (52)$$

Use integration by parts and (52) to obtain

$$\int_0^{\pi/2} f'(2R\sin\theta)\sin^3\theta d\theta = \int_0^{\pi/2} f_0'(2R\sin\theta)\sin^3\theta d\theta - \frac{\delta}{4R^2}$$

$$= \int_0^{\pi/2} f_0'(2R\sin\theta)\sin\theta d\theta - \int_0^{\pi/2} \frac{d}{d\theta}(f_0(2R\sin\theta)) \frac{\sin\theta\cos\theta}{2R}$$

$$= \int_0^{\pi/2} f_0'(2R\sin\theta)\sin\theta + \frac{1}{2R}\int_0^{\pi/2} f_0(2R\sin\theta)d\theta + \frac{\delta}{4R^2} \quad (53)$$

Substituting (53) into (50) yields

$$I_{20} = I_{10} + \frac{\delta}{R\pi}.$$

In summary, we obtain $I_2 = I_1 + \frac{\delta}{R\pi}$ so that

$$\det M = I_1^2 - I_2^2 \sim -\frac{\delta}{R\pi}(2I_1 + \frac{\delta}{R\pi}).$$

It follows that the threshold $\det M = 0$ occurs when $2I_1 + \frac{\delta}{R\pi} = 0$, or

$$4R \int_0^{\pi/2} (Rf_0'(2R\sin\theta)\sin\theta + f_0(2R\sin\theta))\, d\theta + \delta(\ln N + \ln(4/\pi) + \gamma + 1)$$

Solving for $N_c = N$ yields (37). Expanding (37) in δ yields (39).   □

Proof of Proposition 2. We seek a two-ring equilibrium state of radii R_i, R_o, each having the same number of particles. Let

$$R_i = R - \varepsilon; \quad R_o = R + \varepsilon.$$

Then similar to a single ring, and in the limit $N \to \infty$, the radii satisfy

$$0 = \int_0^{\pi/2} d\theta \left[f(2(R-\varepsilon)\sin\theta)2(R-\varepsilon)\sin^2\theta + f\left(2\sqrt{(R^2-\varepsilon^2)\sin^2\theta + \varepsilon^2}\right)\left(2\sin^2(\theta)(R+\varepsilon) - 2\varepsilon\right) \right]$$

$$0 = \int_0^{\pi/2} d\theta \left[f(2(R+\varepsilon)\sin\theta)2(R+\varepsilon)\sin^2\theta + f\left(2\sqrt{(R^2-\varepsilon^2)\sin^2\theta + \varepsilon^2}\right)\left(2\sin^2(\theta)(R-\varepsilon) + 2\varepsilon\right) \right]$$

Define

$$I_1(\varepsilon) := \int_0^{\pi/2} f(2(R+\varepsilon)\sin\theta)2(R+\varepsilon)\sin^2\theta d\theta;$$

$$I_2(\varepsilon) := \int_0^{\pi/2} f\left(\sqrt{4(R^2-\varepsilon^2)\sin^2\theta + 4\varepsilon^2}\right) 4R\sin^2(\theta);$$

$$I_3(\varepsilon) := \int_0^{\pi/2} f\left(\sqrt{4(R^2-\varepsilon^2)\sin^2\theta + 4\varepsilon^2}\right) 4\varepsilon\cos^2(\theta);$$

so that the steady state satisfies

$$I_1(\varepsilon) + I_1(-\varepsilon) + I_2(\varepsilon) = 0; \qquad I_1(\varepsilon) - I_1(-\varepsilon) + I_3(\varepsilon) = 0.$$

We have

$$I_1(\varepsilon) + I_1(-\varepsilon) = 4R\int_0^{\pi/2} f(2R\sin\theta)\sin^2\theta d\theta + O(\varepsilon^2);$$

$$I_1(\varepsilon) - I_1(-\varepsilon) = 2\varepsilon\left\{\int_0^{\pi/2} 4Rf'(2R\sin\theta)\sin^3\theta + \int_0^{\pi/2} f(2R\sin\theta)\sin^2\theta\right\}$$

and we simplify

$$I_2(\varepsilon) \sim \int_0^{\pi/2} f(2R\sin\theta)4R\sin^2\theta + O(\varepsilon^2).$$

For I_3 we split off the singularity to write it as $I_3 = I_{31} + I_{32}$ with

$$I_{31} := 4\varepsilon\int_0^{\pi/2} f_0(2R\sin\theta)\cos^2(\theta); \quad I_{32} := 4\delta\varepsilon\int_0^{\pi/2} \left(4(R^2-\varepsilon^2)\sin^2\theta + 4\varepsilon^2\right)^{-1/2}\cos^2(\theta)$$

Using the asymptotics

$$\int_0^{\pi/2} \left(\sin^2\theta + \varepsilon^2\right)^{-1/2}\cos^2\theta \sim -\ln\varepsilon - 1 + \ln 4 + O(\varepsilon^2\ln\varepsilon)$$

we then obtain

$$I_{32} = 2\delta\frac{\varepsilon}{R}\left(-\ln\frac{\varepsilon}{R} - 1 + \ln 4\right).$$

In summary, we get

$$0 \sim \int_0^{\pi/2} f(2R\sin\theta)\sin^2\theta d\theta; \tag{54}$$

$$0 \sim \int_0^{\pi/2} 4Rf'(2R\sin\theta)\sin^3\theta + 2\int_0^{\pi/2} f_0(2R\sin\theta)\cos^2(\theta) + \frac{\delta}{R}\left(-\ln\frac{\varepsilon}{R} - 1 + \ln 4\right). \tag{55}$$

Next we simplify (55) by using identities (53) and (52); this yields (44), from which (45) follows by expanding in δ. $\qquad\square$

7. **Custom-designer kernels in 2D.** In the previous sections our primary focus was to understand the resulting ground state pattern from a given interaction kernel, f. In this section we consider the inverse problem of, given a particular pattern, can one construct interaction kernel(s) who's ground state will exhibit this pattern? This problem is exceedingly complex and non-unique in general but here we solve the following inverse problem: Consider a co-dimension one ground state which can be approximated by a finite collection of Fourier modes, can one construct an interaction kernel whose ground state will contain the same set of Fourier modes?

In three dimensions, this question was recently solved in full (though non-uniquely) in [37]. In this section, we extend the analysis of [37] to two dimensions. To begin recall that the eigenvalues of the matrix

$$M(m) := \begin{pmatrix} I_1(m) & I_2(m) \\ I_2(m) & I_1(-m) \end{pmatrix}$$

determine the stability of mode m, in that we require strictly negative eigenvalues, except for the zero eigenvalues that result from rotation and translation invariance of the ring steady-state. We now reformulate this matrix using the notation introduced in [38, 37]. For each fixed mode m, we perform a similarity transformation to $M(m)$ to obtain the matrix

$$\Omega(m) := \frac{1}{2} \begin{pmatrix} 1 & 1 \\ -\frac{1}{m} & \frac{1}{m} \end{pmatrix} \begin{pmatrix} I_1(m) & I_2(m) \\ I_2(m) & I_1(-m) \end{pmatrix} \begin{pmatrix} 1 & -m \\ 1 & m \end{pmatrix}.$$

Note that this change of variables does not change the sign of the eigenvalues, so that $\Omega(m)$ characterizes the stability of mode m in exactly the same fashion as $M(m)$ does. By straightforward computation,

$$\Omega(m) := \frac{1}{2} \begin{pmatrix} I_1(m) + I_1(-m) + 2I_2(m) & m(I_1(-m) - I_1(m)) \\ \frac{1}{m}(I_1(-m) - I_1(m)) & I_1(m) + I_1(-m) - 2I_2(m) \end{pmatrix}.$$

First, let $g(s) := f(\sqrt{2s})$ and let $V(s)$ denote a potential, i.e. that $V'(s) = -g(s)$. By applying the change of variables $\eta = 2\theta$ in the definition of the integrals $I_1(m)$ and $I_2(m)$, integrating by parts and using the radius condition for R we discover that

$$I_1(m) + I_1(-m) + 2I_2(m) = \frac{2}{\pi} \int_0^\pi g\left(R^2 - R^2\cos(\eta)\right)(1 - \cos(\eta)\cos(m\eta))\,\mathrm{d}\eta$$
$$+ \frac{2}{\pi} \int_0^\pi R^2 g'\left(R^2 - R^2\cos(\eta)\right)(1 - \cos(\eta))^2(1 + \cos(m\eta))\,\mathrm{d}\eta,$$

$$I_1(-m) - I_1(m) = m\frac{2}{\pi} \int_0^\pi g\left(R^2 - R^2\cos(\eta)\right)(1 - \cos(\eta))\cos(m\eta)\mathrm{d}\eta,$$

$$I_1(m) + I_1(-m) - 2I_2(m) = -\frac{m^2}{R^2}\frac{2}{\pi} \int_0^\pi V\left(R^2 - R^2\cos(\eta)\right)\cos(m\eta)\mathrm{d}\eta.$$

Next, define the auxiliary quantities

$$\alpha = \frac{1}{\pi} \int_0^\pi g\left(R^2 - R^2\cos(\eta)\right) + R^2 g'\left(R^2 - R^2\cos(\eta)\right)(1 - \cos(\eta))^2\,\mathrm{d}\eta,$$
$$g_1(\eta) = R^2 g'\left(R^2 - R^2\cos(\eta)\right)(1 - \cos(\eta))^2 - \cos(\eta)g\left(R^2 - R^2\cos(\eta)\right),$$
$$g_2(\eta) = g\left(R^2 - R^2\cos(\eta)\right)(1 - \cos(\eta)),$$
$$g_3(\eta) = -\frac{1}{R^2}V\left(R^2 - R^2\cos(\eta)\right).$$

These allows us to characterize stability in terms of the Fourier coefficients $\hat{g}_i(m)$ of the auxiliary quantities. That is, the matrix $\Omega(m)$ becomes

$$\Omega(m) := \begin{pmatrix} \alpha + \hat{g}_1(m) & m^2\hat{g}_2(m) \\ \hat{g}_2(m) & m^2\hat{g}_3(m) \end{pmatrix} \tag{56}$$

where

$$\hat{g}_i(m) = \frac{1}{\pi} \int_0^\pi g_i(\eta)\cos(m\eta)\mathrm{d}\eta. \tag{57}$$

Therefore, for a mode $m \geq 2$ to have strictly negative eigenvalues we require that all of

$$\alpha + \hat{g}_1(m) < 0 \quad \hat{g}_3(m) < 0 \quad (\hat{g}_2(m))^2 < (\alpha + \hat{g}_1(m))\,\hat{g}_3(m)$$

simultaneously hold.

Now, let us fix a ring solution with $R = 1$ and turn to the task of destabilizing an odd mode $m = 2n + 1$. For this, we take a kernel

$$f(\sqrt{2s}) = g^{2n+1}(s) := c_0(1+2(1-s))+\frac{2n-1}{2n}(1+c_1)(1-s)^{2n-2}+c_1(1-s)^{2n-1}-(1-s)^{2n} \tag{58}$$

for some choice of coefficients c_0, c_1 that are positive. A simple computation then yields

$$g_3(\eta) = \frac{\cos^{2n+1}(\eta)}{2n+1} - \frac{1}{2n}\left[c_1\cos^{2n}(\eta) + (1+c_1)\cos^{2n-1}(\eta)\right] - c_0\left[\cos(\eta) + \cos^2(\eta)\right].$$

Recalling the standard identities

$$\cos^{2n+1}(\eta) = \frac{1}{2^{2n}}\sum_{k=0}^{n}\binom{2n+1}{k}\cos((2n-2k+1)\eta),$$

$$\cos^{2n}(\eta) = \frac{1}{2^{2n}}\binom{2n}{n} + \frac{1}{2^{2n-1}}\sum_{k=0}^{n-1}\binom{2n}{k}\cos((2n-2k)\eta),$$

and the orthogonality of the $\cos(k\eta), k \in \mathbb{N}$ in $L^2([0,\pi])$ then shows that

$$\hat{g}_3(2n+1) > 0.$$

In other words, the mode $m = 2n+1$ is always unstable, independently of the choice of c_0 and c_1. Moreover, computing the auxiliary quantities shows that each $g_i(\eta)$ is a polynomial in $\cos(\eta)$ of degree at most $2n + 1$. Therefore,

$$\hat{g}_i(m) = 0$$

for all $m > 2n + 1$ by orthogonality and the above identities. In these cases, the matrix $\Omega(m), m > 2n + 1$ has eigenvalues $\lambda = \alpha, 0$. In other words, if $\alpha < 0$ then all modes larger than $2n+1$ are neutrally stable. The goal is then simply to choose c_1 (depending on n) and c_0 (depending on c_1) appropriately so that $g^{2n+1}(s)$ has all modes $m < 2n$ stable as well. When a kernel $g^{2n+1}(s)$ has all modes less than $2n + 1$ stable, mode $2n + 1$ unstable, and all modes greater than $2n + 1$ neutrally stable we shall say $g^{2n+1}(s)$ is a **primitive kernel** for the mode $2n + 1$. Using a kernel as above, we need to check only a finite number of conditions to ensure that a given choice of c_0, c_1 results in a primitive kernel.

For instance, if we choose $(n, c_0, c_1) = (1, 0, 1)$ then it is tedious but routine to check that

$$g^3(s) = 1 + (1 - s) - (1 - s)^2$$

is a primitive kernel for mode 3. Similarly, taking $(n, c_0, c_1) = (2, 0, 1)$ gives a primitive kernel for mode 5,

$$g^5(s) = \frac{3}{2}(1 - s)^2 + (1 - s)^3 - (1 - s)^4.$$

In general, following the methods of [37] would show that in general taking $c_1 = \mathcal{O}(n)$ and $c_0 = \mathcal{O}(c_1/n)$ results in a primitive kernel for mode $2n + 1$, although a complete proof of this fact is well beyond the scope of this work.

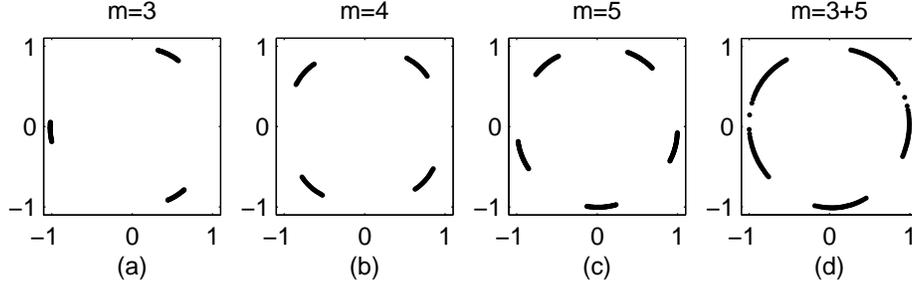FIGURE 4. Steady-states arising from custom-designer kernels using 200 particles. (a) Pure mode $m = 3$ instability with $g = g^3 + 1.1158g^0$. (b) Pure mode $m = 4$ instability with $g = g^4 + 1.3g^0$. (c) Pure mode $m = 5$ with $g = g^5 + 1.3g^0$. (d) Mixed mode $m = 3, 5$ instability with $g = 1.1225g^3 + g^5 + 1.3g^0$.

The primitive kernels for an even mode $2n + 2 \geq 4$ take the form

$$g^{2n+2}(s) = c_0(1+2(1-s))+(1+c_1)(1-s)^{2n-1}+c_1(1-s)^{2n}-\frac{2n+2}{2n+1}(1-s)^{2n+1}; \quad n \geq 1$$

(59)

again for appropriate choices of c_1 (depending on n) and c_0 (depending on c_1). As before,

$$\hat{g}_3(2n) > 0$$

regardless of the choices of c_0, c_1, and $\Omega(m)$ has eigenvalues $\lambda = \alpha, 0$ for all $m > 2n$. Thus, we again have only a finite number of conditions to check to guarantee that a particular choice of c_0, c_1 results in a primitive kernel for the mode $2n$. Again, straightforward calculations show that the choice $(n, c_0, c_1) = (1, 3, 2)$ gives a primitive kernel for mode 4,

$$g^4(s) = 3(1 + 2(1 - s)) + 3(1 - s) + 2(1 - s)^2 - \frac{4}{3}(1 - s)^3.$$

Lastly, we require a kernel that has a ring of radius $R = 1$ as a stable steady state. Using lemma 5.3 in [37], we can prove that

$$g^0(s) = 1 + 2(1 - s) + s^{-\frac{1}{4}} - \mu$$

where

$$\mu = \frac{1}{\pi} \int_0^\pi (1 - \cos x)^{3/4} \, dx \approx 0.93577$$

gives precisely such a kernel. This gives us the final ingredient we need in order to construct kernels with desired instabilities. For instance, if we want a kernel with only mode 3 unstable, we take a primitive kernel $g^3(s)$ for mode 3 and set

$$g(s) = g^3(s) + \epsilon g^0(s).$$

Then for all ϵ sufficiently small, $g(s)$ has a pure mode 3 instability, i.e. mode 3 is unstable and all remaining modes are stable. Indeed, we simply take ϵ small enough so that $\hat{g}(3) > 0$. Figure 4 (a) shows an computed example of this construction for $\epsilon = 1.1158$, i.e. a steady-state resulting from a pure mode 3 instability. Starting with a different primitive kernel and repeating the same procedure gives a kernel with a different, pure instability; for instance modes 4 and 5 are shown in 4 (b,c).

The straightforward generalization of this construction allows us to create kernels with precisely two unstable modes. For concreteness, suppose we want a kernel that has mode 3 and 5 instabilities, while all other modes remain stable. We first take a positive linear combination of a primitive kernel for mode 5 and a stable ring as before,

$$\tilde{g}(s) := g^5(s) + \epsilon_1 g^0(s).$$

As before, provided $\epsilon_1 > 0$ is sufficiently small $\tilde{g}(s)$ has a pure mode 5 instability. We take $\epsilon_1 = 1.3$ as in the previous example. Now, take a primitive kernel $g^3(s)$ for mode 3 and set

$$g(s) = \frac{1}{\epsilon_2} g^3(s) + \tilde{g}(s).$$

Then provided $\epsilon_2 > 0$ is sufficiently small, $g(s)$ will have a mode 3 instability as well. Moreover, as the auxiliary quantities $g_i^3(\eta)$ associated to the primitive kernel $g^3(s)$ are polynomials of degree at most 3 in $\cos(\eta)$, the choice ϵ_2 does not affect the instability of mode 5, no matter how large or small. This yields a kernel that has mode 3 and 5 instabilities, while all other modes remain stable as desired. Figure 4(d) shows an example of such a mixed 3+5 mode steady-state.

We remark that the above construction works for all modes ≥ 3; however it does not work for the mode 2, since the primitive kernel (59) is singular when $n = 0$. It remains an open question whether it is possible to design a kernel which destabilizes mode 2 only.

8. **Second order model.** Until now we have only considered the ground state patterns of the kinematic model (2) for particle interactions, in particular the particles have no independent means of self-motility. Here we extend the stability techniques to the second order models of self-propelled particles such as studied in [20, 10], which incorporate acceleration. We consider the general system

$$x_j' = v_j; \qquad v_j' = g(|v_j|)v_j + \frac{1}{N} \sum_{k,k \neq j} f\left(|x_j - x_k|\right)(x_j - x_k); \qquad (60)$$

the term g corresponds to the self-propulsion and typically has the form [10],

$$g(s) = \alpha - \beta s^2.$$

In [10], a solution consisting of a rotating ring was considered. Such solution has the form

$$x_j = Re^{i\theta} \quad \text{where } \theta = \omega t + 2\pi j/N; \qquad v_j = \omega i Re^{i\theta}.$$

Equating real and imaginary parts, we find that the frequency ω and the radius R satisfy

$$g(\omega R) = 0;$$

$$-\omega^2 = \frac{4}{N} \sum_{k=1}^{N/2} f\left(2R\left|\sin\frac{\pi k}{N}\right|\right) \sin^2\left(\frac{\pi k}{N}\right). \qquad (61)$$

In the continuum limit, (61) becomes

$$-\omega^2 = \frac{4}{\pi} \int_0^{\pi/2} f\left(2R\left|\sin\theta\right|\right) \sin^2\theta d\theta; \qquad g(\omega R) = 0.$$

We now take the perturbation of the form

$$x_j = Re^{i\theta}\left(1 + h_j\right), \quad h_j \ll 1.$$

and we compute,

$$x'_j = Re^{\theta i}\omega i \left(1 + h_j + \frac{h'_j}{i\omega}\right);$$

$$|x'_j| = R\omega \left(1 + \frac{1}{2}\left[h_j + \overline{h_j} + \frac{h'_j}{i\omega} - \frac{\overline{h'_j}}{i\omega}\right]\right);$$

$$g(|v_j|)v_j = Re^{\theta i}g'(R\omega)R\omega\frac{1}{2}\left[i\omega h_j + i\omega\overline{h_j} + h'_j - \overline{h'_j}\right]$$

$$x''_j = Re^{\theta i}\left(-\omega^2 - h_j\omega^2 + 2\omega i h'_j + h''_j\right)$$

so that the linearized equations become

$$-h_j\omega^2 + 2\omega i h'_j + h''_j = g'(R\omega)R\omega\frac{1}{2}\left[i\omega h_j + i\omega\overline{h_j} + h'_j - \overline{h'_j}\right]$$
$$+ \sum_{k,k\neq j} G_1(\phi/2)\left(h_j - e^{i\phi}h_k\right) + G_2(\phi/2)\left(\overline{h_k} - e^{i\phi}\overline{h_j}\right)$$

where G_1 and G_2 are defined in (12) and $\phi = \frac{2\pi(k-j)}{N}$.

As before, we make an ansatz

$$h_j = \xi_+(t)e^{im\theta} + \xi_-(t)e^{-im\theta}, \quad \theta = 2\pi j/N, \quad m \in \mathbb{N}$$

Equating the like terms in $e^{im\theta}$ yields

$$-\xi_+\omega^2 + 2\omega i\xi'_+ + \xi''_+ = A_0\left[i\omega\xi_+ + i\omega\overline{\xi_-} + \xi'_+ - \overline{\xi_-}'\right] + \xi_+I_1(m) + \overline{\xi_-}I_2(m)$$

where I_1 and I_2 are defined in (7, 8) and where

$$A_0 = g'(R\omega)R\omega\frac{1}{2}.$$

Equating the like terms in $e^{-im\theta}$ and taking a conjugate yields

$$-\overline{\xi_-}\omega^2 - 2\omega i\overline{\xi_-}' + \overline{\xi_-}'' = A_0\left[-i\omega\xi_+ - i\omega\overline{\xi_-} - \xi'_+ + \overline{\xi_-}'\right] + \xi_+I_2(m) + \overline{\xi_-}I_1(-m).$$

Setting $\xi'_\pm = \eta_\pm$, we obtain the following linear system:

$$\frac{d}{dt}\begin{pmatrix} \eta_+ \\ \overline{\eta_-} \\ \xi_+ \\ \overline{\xi_-} \end{pmatrix} = \begin{pmatrix} A_0 - 2\omega i & -A_0 & i\omega A_0 + \omega^2 + I_1(m) & i\omega A_0 + I_2(m) \\ -A_0 & A_0 + 2\omega i & -i\omega A_0 + I_2(m) & -i\omega A_0 + \omega^2 + I_1(-m) \\ 1 & 0 & 0 & 0 \\ 0 & 1 & 0 & 0 \end{pmatrix}\begin{pmatrix} \eta_+ \\ \overline{\eta_-} \\ \xi_+ \\ \overline{\xi_-} \end{pmatrix}$$

(62)

The solution to this linear system is given by $\begin{pmatrix} \eta_+ \\ \overline{\eta_-} \\ \xi_+ \\ \overline{\xi_-} \end{pmatrix} = e^{\lambda t}\begin{pmatrix} a \\ b \\ c \\ d \end{pmatrix}$ where λ is an

eigenvalue of the 4x4 matrix in (62). By eliminating c and d we then obtain the following system that the eigenvalue λ must satisfy:
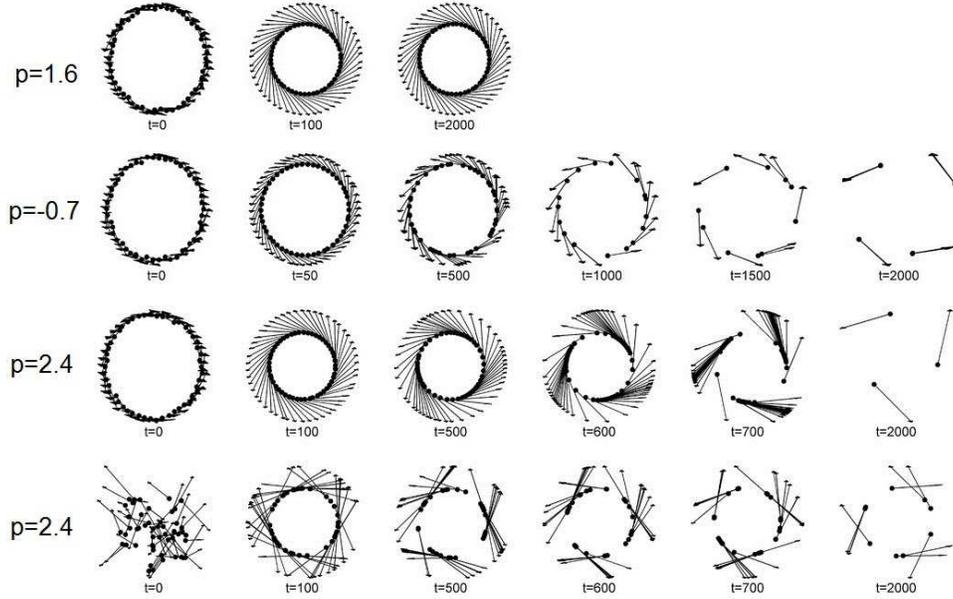
$$\lambda^2 v = M_1 v\lambda + M_0 v$$

FIGURE 5. Dynamics of the 2nd order model (60) with $N = 50$, $g(s) = 1 - s^2$ and $f(r) = -r^p$, with p as indicated. Row 1-3: The initial conditions are taken to be a slight random perturbation of a ring of radius one rotating counterclockwise. Row 4: Initial positions and velocities are taken to be random inside a unit square.

where $v = (a, b)^t$ and where

$$M_1 = \begin{pmatrix} A_0 - 2\omega i & -A_0 \\ -A_0 & A_0 + 2\omega i \end{pmatrix};$$

$$M_0 = \begin{pmatrix} i\omega A_0 + \omega^2 + I_1(m) & i\omega A_0 + I_2(m) \\ -i\omega A_0 + I_2(m) & -i\omega A_0 + \omega^2 + I_1(-m) \end{pmatrix}; \quad A_0 = g'(R\omega)R\omega\frac{1}{2}$$

Example 1. Consider $f(s) = -1$; $g(s) = \alpha - \beta s^2$. Then

$$\omega = 1, \quad R = \sqrt{\alpha/\beta}.$$

Moreover, $I_1(m) = -\frac{4}{\pi}\int_0^{\pi/2}\sin^2((m+1)\theta)d\theta = -1$; $I_2(m) = 0$, $A_0 = -\alpha$. Computing the characteristic polynomial of (62) then yields

$$\lambda\left(\lambda^3 + 2\alpha\lambda^2 + 4\lambda + 4\alpha\right) = 0.$$

Therefore $\text{Re}(\lambda) \leq 0$, by the winding number test. It follows that the ring is stable for all choices of $\alpha, \beta > 0$.

Example 2. Take $f(s) = -as^p$; we will choose the constant a to make $R = \frac{1}{2}$ to simplify the computations. Then a, ω satisfies:

$$\omega^2 = \frac{4a}{\pi}\int_0^{\pi/2}\sin^{2+p}\theta d\theta; \quad \omega = 2\sqrt{\alpha/\beta}.$$

Now we have

$$\int_0^{\pi/2}\sin^{2+p}\theta d\theta = \frac{\sqrt{\pi}}{2}\frac{p+1}{p+2}\frac{\Gamma(\frac{p}{2}+\frac{1}{2})}{\Gamma(\frac{p}{2}+1)}$$
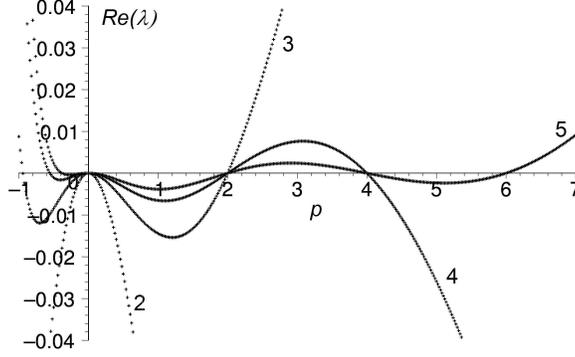
FIGURE 6. The stability with respect to modes $m = 2 \ldots 5$ as a function of p for the rotating ring of Example 2. All modes are stable if and only if $p \in (0, 2)$.

which yields

$$\omega = 2\sqrt{\alpha/\beta}, \quad a = 2\alpha/\beta\sqrt{\pi}\frac{\Gamma(\frac{p}{2} + 1)}{\Gamma(\frac{p}{2} + \frac{1}{2})}\frac{p + 2}{p + 1}, \quad R = \frac{1}{2}.$$

Next we consider the stability. We have

$$I_1(m) = -\frac{4a}{\pi}\left(\frac{p}{2} + 1\right)\int_0^{\pi/2}\sin^p\theta\sin^2((m + 1)\theta)d\theta;$$

$$I_2(m) \sim -\frac{4a}{\pi}\left(\frac{p}{2}\right)\int_0^{\pi/2}\sin^p\theta\left[\sin^2(\theta) - \sin^2(m\theta)\right]d\theta;$$

$$A_0 = -\alpha$$

Figure 6 shows the $\text{Re}(\lambda)$ corresponding to the first few modes $m = 2 \ldots 5$. As p is increased from zero, the instability is first observed when p crosses 2. This instability threshold happens when λ crosses zero at which point $\det(M_0) = 0$ or

$$\omega^4 + \omega^2 I_1(m) + I_1(-m)) + I_1(m)I_1(-m) - I_2(m)^2 + iwA_0(I_1(-m) - I_1(m)) = 0$$

This is only possible if

$$I_1(m) = I_1(-m) \quad \text{and} \quad \omega^4 + \omega^2 2I_1(m) + I_1^2(m) - I_2^2(m) = 0. \tag{63}$$

From Lemma A.1, the condition $I_1(m) = I_1(-m)$ is satisfied if and only if p is even and $\frac{p}{2} < m - 2$. In this case we obtain

$$I_1(m) = I_1(-m) = -\alpha/\beta\frac{(p + 2)^2}{p + 1}; \quad I_2(m) = -\alpha/\beta\frac{p^2}{p + 1} \qquad p \text{ is even}$$

and moreover the second condition in (63) is then automatically satisfied.

Another type of instability occurs when $p < 0$, as illustrated in Figure 6. This is due to a Hopf bifurcation. For example, taking $\alpha, \beta = 1$, the mode $m = 3$ undergoes a Hopf bifurcation when p is decreased past $p_h \approx -0.9405$ with $\lambda \approx 0.08044i$. All higher modes m also undergo a Hopf bifurcation for $p < 0$. In fact, **the ring is high wave number unstable for $p < 0$** and breaks up, as confirmed via numerical simulations.

9. **Discussion.** We investigated the stability of a ring pattern in a two-dimensional aggregation model. We extended the stability theory to the rotating ring state for the second-order models of self-propelled particles. Some of the results were first published in [17] without proofs. Here we provide the detailed derivations. We also extended the results of [37, 38] on custom kernels from three to two dimensions.

There are two basic types of instabilities that can occur: a low mode instability which leads to curve deformation, and a high-mode instability which can lead to a complete disintegration of the ring. We analyzed both types of instabilities in detail. We clarified the shape of the bifurcation corresponding to a low-mode instability. Using weakly nonlinear analysis, we derived a set of conditions for when such a bifurcation is a pitchfork.

The high-mode instability depends on the local behaviour of the force $F(r)$ near $r = 0$. If the leading order behaviour is $F(r) \sim ar^p$ as $r \to 0$ where $a > 0$, then we show that a necessary (but not sufficient) conditions for stability of a ring is that $p > 0$. Recently, it was shown in [1] that the Hausdorff dimension of the steady state in two dimensions is at least $1 - p$ provided that $-1 \le p \le 1$ which is consistent with our analysis of the high-mode perturbations. The threshold case $p = 0$ is particularly interesting: as we show in Proposition 1, in this case it is possible for a *discrete* ring of N particles to be stable for very large N, although it is unstable in the continuum limit. Moreover as N is increased multiple "bifurcations" in N are observed, from single to multiple rings to a continuum "thin annulus" (Figure 3). The density of the resulting annulus was recently analyzed in [16]; it was shown that in the threshold case $p = 0$, the density blows up near the boundaries of the annulus.

A key open question is to study the stability of co-dimension two patterns (for stability of co-dimension zero patterns consisting of "black holes", see [12] in one dimension and [16, 31] in two dimensions). Many such steady states can be constructed analytically; see for example [16]. Unlike the the ring patterns, there is no known unstable co-dimension two patterns; they are difficult to compute numerically since the simulations typically rely on the ODE particle formulation which will diverge away from any unstable pattern.

For the second-order models, double-mill formations are commonly observed especially when the repulsion is relatively weak at the origin [10]. It is an open question to analyze the stability of such double-mills.

Appendix A. **The key integral.**

Lemma A.1. *Let*

$$I(p,m) := \int_0^{\pi/2} \sin^p(x) \sin^2(mx) dx; \quad with \quad p > -3, \quad m \in \mathbb{N}.$$

This integral has the following representations.

1. *If $p \neq -1$ and $\frac{p}{2} \notin \mathbb{N}$ then*

$$I(p,m) = \frac{\sqrt{\pi}}{4} \frac{\Gamma\left(\frac{p}{2}+\frac{1}{2}\right)}{\Gamma(\frac{p}{2}+1)} \left[1 - (-1)^m \frac{\Gamma(\frac{p}{2}+1)^2}{\Gamma(\frac{p}{2}+1+m)\Gamma(\frac{p}{2}+1-m)} \right] \tag{64}$$

$$= \frac{\sqrt{\pi}}{4} \frac{\Gamma\left(\frac{p}{2}+\frac{1}{2}\right)}{\Gamma(\frac{p}{2}+1)} \left[1 + \frac{\sin\left(\pi\frac{p}{2}\right)\Gamma(\frac{p}{2}+1)^2}{\pi} \frac{\Gamma\left(m-\frac{p}{2}\right)}{\Gamma(m+\frac{p}{2}+1)} \right] \tag{65}$$

$$\sim \frac{\sqrt{\pi}}{4} \frac{\Gamma\left(\frac{p}{2}+\frac{1}{2}\right)}{\Gamma(\frac{p}{2}+1)} \left[1 + \frac{\sin\left(\pi\frac{p}{2}\right)\Gamma(\frac{p}{2}+1)^2}{\pi} m^{-p-1} \right] \quad as\ m \to \infty \tag{66}$$

2. *If $p = -1$ then*

$$I(-1,m) \sim 2\log m + O(1) \quad as\ m \to \infty \tag{67}$$

3. *If $\frac{p}{2} \in \mathbb{N}$ then*

$$I(p,m) = \begin{cases} \dfrac{\sqrt{\pi}}{4} \dfrac{\Gamma\left(\frac{p}{2}+\frac{1}{2}\right)}{\Gamma(\frac{p}{2}+1)}, & if\ m > \dfrac{p}{2} \\ \dfrac{\sqrt{\pi}}{4} \dfrac{\Gamma\left(\frac{p}{2}+\frac{1}{2}\right)}{\Gamma(\frac{p}{2}+1)} \left[1 - (-1)^m \dfrac{\Gamma(\frac{p}{2}+1)^2}{\Gamma(\frac{p}{2}+1+m)\Gamma(\frac{p}{2}+1-m)} \right], & otherwise \end{cases} . \tag{68}$$

Proof. Let $s = (\sin(x))^2$ so that the integral becomes

$$I(p,m) = \frac{1}{2}\int_0^1 s^{p/2-1/2}(1-s)^{-1/2}\sin^2(m\arcsin s^{1/2})ds.$$

Next, we have the following identity:

$$\sin^2(m\arcsin s^{1/2}) = \frac{1}{2}\left[1 - {}_2F_1\left(\begin{array}{c} m,-m \\ 1/2 \end{array} ;s \right) \right]$$

and write $I(p,m) = \frac{1}{4}I_1 - \frac{1}{4}I_2$ where

$$I_1 = \int_0^1 s^{p/2-1/2}(1-s)^{-1/2}ds; \qquad I_2 = \int_0^1 s^{p/2-1/2}(1-s)^{-1/2}{}_2F_1\left(\begin{array}{c} m,-m \\ 1/2 \end{array} ;s \right) ds.$$

Note that

$$I_1 = \int_0^1 s^{p/2-1/2}(1-s)^{-1/2} = \frac{\Gamma\left(\frac{p}{2}+\frac{1}{2}\right)\Gamma(\frac{1}{2})}{\Gamma(\frac{p}{2}+1)}.$$

To evaluate I_2, we make use of the following fundamental relationship (Euler's transform) [28]:

$$\int_0^1 t^{c-1}(1-t)^{d-c-1}{}_AF_B\left(\begin{array}{c} a_1,\ldots,a_A \\ b_1,\ldots,b_B \end{array} ;tz \right) = \frac{\Gamma(c)\Gamma(d-c)}{\Gamma(d)}{}_{A+1}F_{B+1}\left(\begin{array}{c} a_1,\ldots,a_A,c \\ b_1,\ldots,b_B,d \end{array} ;z \right). \tag{69}$$

It follows that

$$I_2 = \frac{\Gamma(\frac{p}{2}+\frac{1}{2})\Gamma(\frac{1}{2})}{\Gamma(\frac{p}{2}+1)}{}_3F_2\left(\begin{array}{c} m,-m,\ \frac{p}{2}+\frac{1}{2} \\ 1/2,\ \frac{p}{2}+1 \end{array} ;1 \right).$$

Next, we apply the Saalschütz Theorem [5] which states that if Saalschützian relation

$$e + f = a + b + 1 - n \quad and\ \ n \in \mathbb{N}^+, \tag{70}$$

holds, then the following identity is true:

$$_3F_2\left(\begin{array}{c} a,b,-n \\ e,f \end{array};1\right) = \frac{(e-a)_n\,(f-a)_n}{(e)_n(f)_n} \tag{71}$$

where

$$(a)_n = a(a+1)(a+2)\ldots(a+n-1) = \Gamma(a+n)/\Gamma(a).$$

It follows that

$$_3F_2\left(\begin{array}{c} m,-m,\frac{p}{2}+\frac{1}{2} \\ 1/2,\frac{p}{2}+1 \end{array};1\right) = \frac{\Gamma(1/2)^2\Gamma(\frac{p}{2}+1)^2}{\Gamma(\frac{1}{2}-m)\Gamma(\frac{p}{2}+1-m)\Gamma(\frac{1}{2}+m)\Gamma(\frac{p}{2}+1+m)}.$$

Using the identity

$$\Gamma(z)\Gamma(-z) = \frac{-\pi}{\sin(\pi z)\,z}$$

and the fact that m is an integer, we get

$$I_2 = (-1)^m \frac{\Gamma(\frac{p}{2}+1)\Gamma(\frac{p}{2}+\frac{1}{2})\Gamma(\frac{1}{2})}{\Gamma(\frac{p}{2}+1+m)\Gamma(\frac{p}{2}+1-m)}.$$

Putting all together we obtain (64, 65, 68).

Asymptotics, $p \neq -1$: First, note that

$$\Gamma(\frac{p}{2}+1+m)\Gamma(\frac{p}{2}+1-m) = -\pi\frac{\Gamma(m+\frac{p}{2}+1)}{\Gamma\left(m-\frac{p}{2}-1\right)}\frac{(-1)^m}{\sin\left(\pi\frac{p}{2}\right)\left(m-\frac{p}{2}-1\right)}.$$

Now using Sterling's identity, we have

$$\frac{\Gamma(m+\frac{p}{2}+1)}{\Gamma\left(m-\frac{p}{2}-1\right)} \sim m^{p+2} \quad \text{as } m \to \infty$$

This yields (66).

For the asymptotics result for $p = -1$: We write

$$\int_0^{\pi/2} \frac{\sin^2(mx)}{\sin(x)}dx = \int_0^{\pi/2} \frac{\sin^2(mx)}{x}dx + \int_0^{\pi/2} \sin^2(mx)\left(\frac{1}{\sin(x)} - \frac{1}{x}\right)dx.$$

The second integral on the right hand side is bounded independent of m. The first integral is estimated as

$$\int_0^{\pi/2} \frac{\sin^2(mx)}{x}dx = \int_0^{m\pi/2} \frac{\sin^2 y}{y}dy \sim \frac{1}{2}\ln(m) \text{ as } m \to \infty$$

(to see the last estimate, note that $\int_1^{m\pi/2} \frac{\sin^2 y}{y}dy = \int_1^{m\pi/2} \frac{1-\sin(2y)}{2y}dy = \frac{1}{2}\ln m + O(1)$ as $m \to \infty$; on the other hand, $\int_0^1 \frac{\sin^2 y}{y}dy$ is bounded). This proves (67). ∎

REFERENCES

[1] D. Balague, J. A. Carrillo, T. Laurent and G. Raoul, *Dimensionality of local minimizers of the interaction energy*, submitted.

[2] A. J. Bernoff and C. M. Topaz, *A primer of swarm equilibria*, SIAM J. Appl. Dyn. Syst. **10** (2011), 212250.

[3] A. L. Bertozzi, J. A. Carrillo and T. Laurent, *Blowup in multidimensional aggregation equations with mildly singular interaction kernels*, Nonlinearity **22** (2009), 683-710.

[4] A. L. Bertozzi, T. Laurent and J. Rosado, *L^p Theory for the Multidimensional Aggregation Equation*, Commun. Pur. Appl. Math. **64** (2011), 45-83.

[5] J.L. Burchnall and A. Lakin, *The theorems of Saalschütz and Dougall*, Quart. J. Math. **2** (1950), 161-166.

[6] S. Camazine, J.-L. Deneubourg, N. R. Franks, J. Sneyd, G. Theraulaz and E. Bonabeau, *"Self-Organization in Biological Systems"*, Princeton Univ. Press, Princeton, 2003.

[7] I. D. Couzin, J. Krauss, N. R. Franks and S. A. Levin, *Effective leadership and decision-making in animal groups on the move*, Nature **433** (2005), 513-516.

[8] P. Degond and S. Motsch, *Large scale dynamics of the persistent turning walker model of fish behavior*, Journal of Statistical Physics, **131** (2008), 989-1021.

[9] A M. Delprato, A. Samadani, A. Kudrolli and L. S. Tsimring, *Swarming Ring Patterns in Bacterial Colonies Exposed to Ultraviolet Radiation*, Phys. Rev. Lett. **87** (2001).

[10] M. R. D'Orsogna, Y. L. Chuang, A. L. Bertozzi and L. S. Chayes, *Self-Propelled Particles with Soft-Core Interactions: Patterns, Stability, and Collapse*, Phys. Rev. Lett. **96** (2006).

[11] L. Edelstein-Keshet, J. Watmough and D. Grunbaum, *Do travelling band solutions describe cohesive swarms? An investigation for migratory locusts*, J. Math. Bio. **36** (1998), 515-549.

[12] K. Fellner and G. Raoul, *Stable stationary states of non-local interaction equations*, Math. Models Methods Appl. Sci., **20** (2010), 2267–2291.

[13] R C Fetecau and Y Huang and T Kolokolnikov, *Swarm dynamics and equilibria for a nonlocal aggregation model*, Nonlinearity **24** (2011), 2681-2716.

[14] S. A. Kaufmann, *"The Origins of Order: Self-Organization and Selection in Evolution"*, Oxford University Press, New York, 1933.

[15] E. F. Keller and L. A. Segel, *Model for chemotaxis*, J. Theo. Bio. **30** (1971), 225-234.

[16] T. Kolokolnikov, Y. Huang and M. Pavlovski, *Singular patterns for an aggregation model with a confining potential*, Physica D special issue on particle models, to appear.

[17] T. Kolokolnikov, H. Sun, D. Uminsky and A. L. Bertozzi, *Stability of ring patterns arising from two-dimensional particle interactions*, Phys. Rev. E Rapid. Comm. **84** (2011).

[18] T. Laurent, *Local and Global Existence for an Aggregation Equation*, Communications in Partial Differential Equations **32** (2007), 1941-1964.

[19] A. J. Leverentz, C. M. Topaz and A. J. Bernoff, *Asymptotic Dynamics of Attractive-Repulsive Swarms*, SIAM J. Appl. Dyn. Syst. **8** (2009), 880-908.

[20] H. Levine, W-J Rappel and I. Cohen, *Self-organization in systems of self-propelled particles*, Phys. Rev. E **63** (2000).

[21] R. Lukemana, Y-X Lib and L. Edelstein-Keshet, *Inferring individual rules from collective behavior*, P. Natl. Acad. Sci. USA **10** (2010).

[22] A. Mogilner , L. Edelstein-Keshet , *A non-local model for a swarm*, J. Math. Biol., **38** (1999), 534-570.

[23] A. Mogilner, L. Edelstein-Keshet, L. Bent, A. Spiros, *Mutual interactions, potentials, and individual distance in a social aggregation*, J. Math. Bio. **47** (2003), 353-389.

[24] S. Motsch and E. Tadmor, *A New Model for Self-organized Dynamics and Its Flocking Behavior*, Journal of Statistical Physics, **114** (2011), 923-947.

[25] J. K. Parrish and L. Edelstein-Keshet, *Complexity, Pattern, and Evolutionary Trade-Offs in Animal Aggregation*, Science **284** (1999), 99-101.

[26] I. Prigogine, *"Order Out of Chaos"*, Bantam, New York, 1984.

[27] I. Riedel, K. Kruse and J. Howard, *A Self-Organized Vortex Array of Hydrodynamically Entrained Sperm Cells*, Science **309** (2005), 300-303.

[28] L.J. Slater, *"Generalized Hypergeometric Functions"*, Cambridge University Press, Cambridge, England, 1966.

[29] J. Strefler, U. Erdmann and L. Schimansky-Geier, *Swarming in three dimensions*, Phys. Rev. E **78** (2008).

[30] H. Sun, D. Uminsky and A. L. Bertozzi, *A Generalized Birkhoff - Rott Equation for Two-dimensional Active Scalar Problems*, SIAM J. Appl. Math. **72** (2012), 382-404.

[31] H. Sun, D. Uminsky and A. L. Bertozzi, *Stability and clustering of self-similar solutions of aggregation equations*, J. Math. Phys. Special Issue on Incompressible Fluids, Turbulence and Mixing, **53** (2012).

[32] C. M. Topaz, A. J. Bernoff, S. Logan and W. Toolson, *A model for rolling swarms of locusts*, The European Physical Journal - Special Topics **157** (2008), 93-109.

[33] C. M. Topaz and A. L. Bertozzi, *Swarming Patterns in a Two-Dimensional Kinematic Model for Biological Groups*, SIAM J. Appl. Dyn. Syst. **65** (2004), 152-174.

[34] L. Tsimring, H. Levine, I. Aranson, E. Ben-Jacob, I. Cohen, O. Shochet and W. N. Reynolds, *Aggregation Patterns in Stressed Bacteria*, Phys. Rev. Lett. **75** (1995), 1859-1862.

[35] A. M. Turing, *The chemical basis of morphogenesis*, Phil. Trans. Roy. Soc. Lond. B, **237** (1952), 37-72.

[36] T. Vicsek, A. Czirók, E. Ben-Jacob, I. Cohen and O. Shochet, *Novel Type of Phase Transition in a System of Self-Driven Particles*, Phys. Rev. Lett., **75** (1995), 1226–1229.

[37] J. H. von Brecht and D. Uminsky, *On Soccer Balls and Linearized Inverse Statistical Mechanics*, Journal of Nonlinear Science, (2012), 1-25.

[38] J. H. von Brecht, D. Uminsky, T. Kolokonikov and A. L. Bertozzi, *Predicting pattern formation in particle interactions*, Mathematical Models and Methods in Applied Sciences, **22** (2012).

E-mail address: `bertozzi@math.ucla.edu`
E-mail address: `jub@math.ucla.edu`
E-mail address: `tkolokol@mathstat.dal.ca`
E-mail address: `huiprobable@math.ucla.edu`
E-mail address: `duminsky@usfca.edu`